PCCP

Rate coefficient for the $BrO + HO_2$ reaction at 298 K

William J. Bloss,† David M. Rowley,‡ R. Anthony Cox* and Roderic L. Jones

Centre for Atmospheric Science, University of Cambridge, University Chemical Laboratories, Lensfield Road, Cambridge, UK CB2 1EW. E-mail: w.bloss@chemistry.leeds.ac.uk; d.m.rowley@ucl.ac.uk; rac26@cus.cam.ac.uk; rlj1001@cus.cam.ac.uk

Received 14th February 2002, Accepted 30th April 2002
First published as an Advance Article on the web 17th June 2002

The kinetics of the $BrO + HO_2$ reaction (1) have been studied using the technique of flash photolysis/time resolved UV absorption spectroscopy. BrO and HO_2 radicals were generated *via* the $Br + O_3$ and $Cl + CH_3OH/O_2$ methods respectively. The rate coefficient for the reaction was found to be $k_1 = (2.35 \pm 0.82) \times 10^{-11}$ molecule^{-1} cm^3 s^{-1} at 298 K and 760 Torr O_2. Uncertainty limits correspond to combined 2 standard deviation statistical variation and systematic factors. This result is briefly compared with previous determinations of k_1. A study of the enhancement of the HO_2 self-reaction rate in the presence of methanol was also performed, with the observed second-order loss rate coefficient given by $k_{obs} = (2.9 \times 10^{-12} + \alpha\beta[CH_3OH])/(1 + \alpha[CH_3OH])^2$, with $\alpha = (6.15 \pm 0.90) \times 10^{-19}$ molecule^{-1} cm^3 and $\beta = (3.2 \pm 0.5) \times 10^{-11}$ molecule^{-1} cm^3 s^{-1} at 298 K and 760 Torr O_2, for $[CH_3OH] \leqslant 5.5 \times 10^{17}$ molecule cm^{-3}.

1. Introduction

Halogen species are known to play a key role in the destruction of stratospheric ozone. Such destruction occurs through catalytic cycles, in which the active species are regenerated, permitting trace concentrations of radicals (parts per trillion) to influence much higher ozone concentrations. Knowledge of the kinetic and photochemical parameters describing the reactions which comprise such cycles is required in order to understand and model atmospheric ozone concentrations.

Yung *et al.*[1] proposed that the $BrO + HO_2$ reaction could initiate an ozone destruction cycle, in which the synergistic coupling between the bromine and odd-hydrogen families leads to formation of HOBr. Subsequent solar photolysis of HOBr and reactions with ozone complete the cycle, reactions (1a)–(4). A feature of this cycle is that it does not require the presence of atomic oxygen; the $BrO + HO_2$ cycle is therefore of particular significance in the lower stratosphere.

$$BrO + HO_2 \rightarrow HOBr + O_2 \quad (1a)$$

$$HOBr + h\nu \rightarrow OH + Br \quad (2)$$

$$OH + O_3 \rightarrow HO_2 + O_2 \quad (3)$$

$$Br + O_3 \rightarrow BrO + O_2 \quad (4)$$

$$\text{Net: } 2O_3 \rightarrow 3O_2$$

Reaction (1a) limits the rate of this cycle in the mid-latitude sunlit lower stratosphere. The first measurement of k_1 was performed by Cox and Sheppard,[2] who obtained a value of 5×10^{-12} molecule^{-1} cm^3 s^{-1} at 298 K, indicating, assuming a negligible negative temperature dependence, that the reaction was of little importance to stratospheric chemistry. Subsequently, Poulet *et al.*[3] and Bridier *et al.*[4] measured values of 3.3×10^{-11} and 3.4×10^{-11} molecule^{-1} cm^3 s^{-1} respectively for k_1 at 298 K, indicating that the $BrO + HO_2$ cycle was of potential atmospheric importance. These and more recent determinations[5–9] of k_1 (at 298 K) are listed in Table 1. There is considerable disagreement over the value of k_1 at 298 K, with the lowest and highest reported values for k_1 at 298 K varying by a factor of 6. The temperature dependence of reaction (1) is better constrained, with E/R values of $-(580 \pm 100)$,[5] $-(520 \pm 80)$,[6] $-(536 \pm 206)$[7] and $-(385 \pm 60)$[9] K reported. A major uncertainty in the kinetics of reaction (1) is the A-factor, best determined by the rate coefficient at 298 K.

On the basis of the recommendation of DeMore *et al.*[10] (k_1, 298 K $= 2.1 \times 10^{-11}$ molecule^{-1} cm^3 s^{-1}) Lary[11] calculates the $BrO + HO_2$ cycle to be one of the most effective gas-phase ozone destruction cycles in the lower stratosphere, of comparable importance to the NO/NO_2 cycle below 24 km altitude. The $BrO + HO_2$ reaction thus makes a substantial contribution to mid-latitude, lower stratosphere ozone destruction, and to the enhanced efficiency (on a molecule by molecule basis) of bromine with respect to chlorine bearing molecules for ozone loss.[12]

HOBr is the only product of reaction (1) which has been observed; however an alternative channel forming HBr could occur:

$$BrO + HO_2 \rightarrow HBr + O_3 \quad (1b)$$

Even a small (1–2%) flux of the $BrO + HO_2$ reaction through this channel would have a very significant effect upon modelled atmospheric HBr concentrations, and indeed upon the calculated ozone depletion potentials of bromine source gases.[11] Larichev *et al.*[5] determined an upper limit of 1.5% for the production of $HBr + O_3$ from $BrO + HO_2$ at 298 K, obtained from their detection limit for O_3. Subequently Bedjanian *et al.*[9] lowered the upper limit for $HBr + O_3$ formation to 0.4% at 298 K. Mellouki *et al.*[13] studied the reverse reaction ($HBr + O_3$), and concluded from thermodynamic arguments that occurrence of channel (1b) accounted for less than 0.01% of the total reaction. *Ab initio* studies[14] also indicate that HBr formation is not energetically facile.

The $BrO + HO_2$ cycle may also be of importance in the Marine Boundary Layer (MBL). Vogt *et al.*[15] have proposed a

† Present address: School of Chemistry, University of Leeds, Woodhouse Lane, Leeds, UK LS2 9JT.
‡ Present address: Christopher Ingold Laboratories, University College London, 20 Gordon Street, London, UK WC1H 0AJ.

Table 1 Reported measurements of the $BrO + HO_2$ reaction rate coefficient k_1 at 298 K

Authors	Date	k_1 (298 K)/10^{-11} molecule^{-1} cm^3 s^{-1}	Technique[a]
Cox and Sheppard[2]	1982	$0.5^{+0.5}_{-0.3}$	MM/UV
Poulet *et al.*[3]	1992	3.3 ± 0.5	DF/MS
Bridier *et al.*[4]	1993	3.4 ± 1.0	FP/UV
Larichev *et al.*[5]	1995	3.3 ± 0.5	DF/MS
Elrod *et al.*[6]	1996	1.4 ± 0.3	TDF/MS
Li *et al.*[7]	1997	1.9 ± 0.6	DF/MBMS
Cronkhite *et al.*[8]	1998	2.0 ± 0.6	LFP/UV/TDLS
Bedjanian *et al.*[9]	2001	3.1 ± 0.8	DF/MBMS
DeMore *et al.*[10]	1997	2.1 ± 1.5	Evaluation
This Work	2002	2.35 ± 0.82	FP/UV

[a] MM = molecular moduation; UV = ultraviolet/visible absorption detection; DF = discharge flow; MS = mass spectrometric detection; FP = flash photolysis; TDF = turbulent discharge flow; MBMS = molecular beam mass spectrometry; LFP = laser flash photolysis; TDLS = tunable diode laser spectroscopy.

mechanism for the autocatalytic release of bromine in the form HOBr from sea salt aerosol. Their calculations suggest that this mechanism could generate up to 35 pptv of HOBr in the MBL, leading to gas-phase ozone loss through reactions (1a)–(4) which could account for 5–40% of the total chemical loss of O_3 in the MBL.

This work describes a study of the room-temperature rate coefficient for the $BrO + HO_2$ reaction using the technique of flash photolysis with time-resolved UV-absorption spectroscopy, employing a CCD detection system.

2. Approach

For the principal kinetic experiments, BrO and HO_2 radicals were generated following the broadband photolysis of bromine and chlorine in the presence of excess ozone, methanol and oxygen:

$$Br_2 + h\nu \rightarrow 2Br \quad (5)$$

$$Cl_2 + h\nu \rightarrow 2Cl \quad (6)$$

$$Br + O_3 \rightarrow BrO + O_2 \quad (4)$$

$$Cl + CH_3OH \rightarrow HCl + CH_2OH \quad (7)$$

$$CH_2OH + O_2 \rightarrow HO_2 + HCHO \quad (8)$$

Several secondary chemical reactions occurred in the $BrO + HO_2$ reaction system. Of these, the $BrO + BrO$ and $HO_2 + HO_2$ reactions were the most significant (as demonstrated in the sensitivity study section):

$$BrO + BrO \rightarrow 2Br + O_2 \quad (9a)$$

$$\rightarrow Br_2 + O_2 \quad (9b)$$

$$HO_2 + HO_2(+M) \rightarrow H_2O_2 + O_2(+M) \quad (10)$$

The BrO self-reaction has been studied in detail recently in this laboratory[16] and elsewhere. The HO_2 self-reaction has also been the subject of many previous studies, and the rate of reaction (10) is known to increase in the presence of polar molecules such as water, ammonia and methanol.[17] The rate enhancement is believed to result from the formation of a hydrogen-bonded complex with the HO_2 radical, which can act as a chaperone enhancing the rate of formation of the $(HO_2)_2$ intermediates which subsequently decompose to $H_2O_2 + O_2$. Linear increases in the rate of the HO_2 self-reaction have been observed with respect to the concentration of water[18] and methanol;[17] for ammonia however a fall-off in the rate enhancement has been observed at high $[NH_3]$.[19] In the $BrO + HO_2$ experiments, relatively high methanol concentrations were used (to minimise the fraction of the Cl atoms that reacted with ozone). These concentrations exceeded those at which reaction (10) had been investigated previously; a study of the HO_2 self-reaction in the presence of methanol was therefore conducted to establish the dependence of k_{10} upon the methanol concentrations used.

In the full $BrO + HO_2$ kinetic experiments, the concentration of BrO radicals was monitored as a function of time to obtain kinetic information. It was not possible to obtain HO_2 concentrations reliably by the same method, due to the contaminating absorption arising from the significant concentrations of O_3 required to stoichiometrically convert Br atoms to BrO radicals. The initial concentration of HO_2 radicals generated *via* reactions (6), (7) and (8) was however constrained: An actinometric calibration of Cl_2 photolysis (and hence Cl atom generation and subsequent HO_2 production) was performed by monitoring the production of methylperoxy radicals in separate back-to-back experiments employing the photolysis of (known) concentrations of Cl_2 in the presence of O_2 and CH_4.

The apparatus details and analysis methodology are briefly described in the next section, followed by accounts of the experiments performed to study

(a) the $HO_2 + HO_2$ methanol enhancement,
(b) the Cl_2 photolysis/initial HO_2 calibration and
(c) the full $BrO + HO_2$ kinetic experiments.

Finally, the sensitivity study performed to evaluate the fitting model used in (c) is described, followed by a discussion of the results obtained and comparison with other studies.

3. Experimental details

The $BrO + HO_2$ reaction system was studied using the technique of broadband flash photolysis coupled with time-resolved UV-visible absorption spectroscopy. Charge-coupled-device (CCD) detection was used to monitor the photolysis-initiated evolution and decay of chemical species. The apparatus has been described in detail previously,[16] therefore only a brief description is given here. A schematic diagram of the apparatus is shown in Fig. 1.

Precursor gas mixtures were prepared in a gas manifold using stainless-steel mass flow controllers, and flowed continuously through a 1 m long jacketed quartz reaction cell. The reaction cell was thermostatted at 298 ± 3 K. Cell pressure was measured with a capacitance manometer.

Reactions were initiated using a 50 Torr Xe flashlamp mounted adjacent and parallel to the reaction cell. The lamp was operated at 19–23 kV discharge voltages, corresponding to pulse energies of the order of 500 J, with a pulse duration (FWHM) of 14 μs. The flashlamp was enclosed in a Pyrex jacket to attenuate short wavelength ($\lambda < 280$ nm) emission and minimise O_3 photolysis within the reaction cell. The Pyrex jacket and reaction cell chamber were continuously purged with N_2.

Concentrations of precursor gases, reactants, intermediate species and products were monitored using UV-visible absorption spectroscopy. Analysis light from either a 30 W continuous output xenon arc lamp or a 30 W deuterium lamp was collimated and passed along the long axis of the reaction cell. The analysis light beam was then focused onto the entrance slit of a 0.25 m focal length astigmatic Czerny-Turner spectrograph, fitted with three interchangeable diffraction gratings having 150, 300 and 600 grooves mm^{-1} respectively. Wavelength-resolved analysis light from the spectrograph was imaged across the top of the CCD detector.

The CCD comprises an array of 1152 rows by 298 columns of light sensitive pixels, which convert incident light into

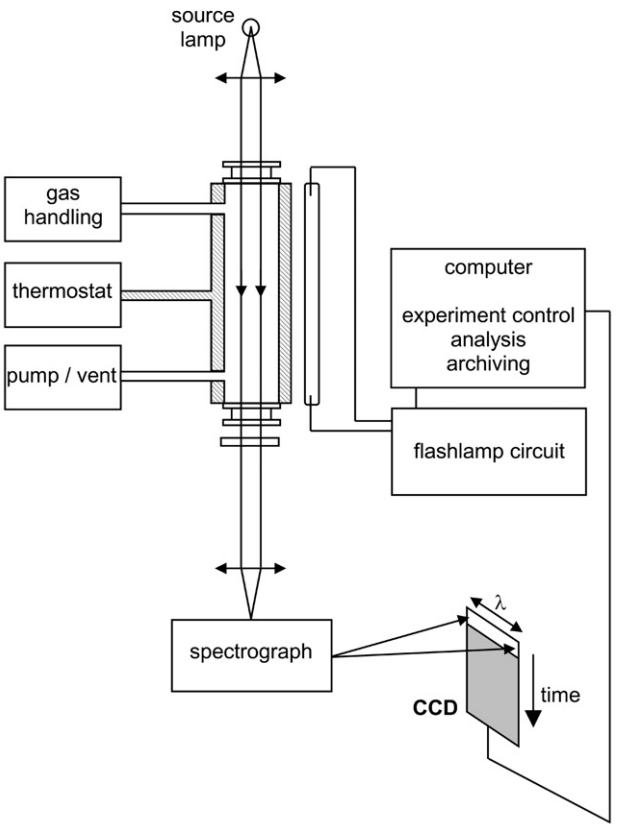

Fig. 1 Schematic diagram of the flash photolysis apparatus.

photocharge. The device also has the facility to shift the photocharge rapidly and efficiently from row to row along the long axis of the array. The CCD was thus positioned with the short axis of the device in the dispersive focal plane of the spectrograph, perpendicular to the axis of fast charge transfer. The top 31 rows of pixels only were illuminated, and rows of photocharge, representing spectra of the transmitted analysis light intensity, were shifted down the device into an optically masked region. When the top row of charge had traversed the entire device, charge transfer ceased and stored photocharge was read off and transferred to a PC for analysis. In this way, up to 1152 sequential transmission spectra of the reaction cell could be recorded. Charge transfer rates of up to 1 MHz per row (1 μs per spectrum) were attainable. Wavelength coverage of up to 130 nm per spectrum was possible, depending upon the diffraction grating used. The spectrograph was regularly wavelength calibrated and the spectral resolution determined using the spectral emission lines from a low-pressure mercury lamp.

Absorption spectra of precursor gas mixtures were obtained from the ratio of the resolved analysis light intensity in the presence (I_t) and absence (I_0) of the gas mixture, according to Beer's law:

$$A_\lambda = \ln\{I_{0,\lambda}/I_{t,\lambda}\} \quad \text{(i)}$$

In kinetic experiments the flashlamp pulse was initiated during the charge transfer process and time-resolved spectra were calculated using an average pre-photolysis intensity as I_0; the spectra so-obtained therefore show changes in the absorbance of the reaction mixture as a result of the photolysis pulse and subsequent chemistry.

Absorption spectra were analysed by numerically fitting reference cross sections for the species of interest to the observed spectra over an appropriate wavelength range. Thus, in kinetic experiments, a spectrum was analysed to determine species concentrations at each time point. Where the species of interest had spectrally structured absorption features, a 'differential' spectral fitting technique was employed. This involved the high-pass filtering of both the observed spectrum and the reference cross-sections, with fitting of the resulting structure using a linear least-squares method.[16] The kinetic traces so obtained were analysed using a model of the reaction system constructed in the numerical integration package FACSIMILE,[20] as described later.

Cl_2 (5.2% in N_2, BOC), CH_4 (99.995%, MG Distillers) and O_2 (99.998%, MG Distillers) were used as supplied; CH_3OH (Fisher Scientific, 99.99%) was purified through several freeze–pump–thaw cycles. The Cl_2 and O_2 were introduced into the gas manifold through mass-flow controllers. CH_3OH was entrained in a controlled flow of N_2 passed through a bubbler immersed in cold water, the temperature of which was held constant to ensure a known CH_3OH vapour pressure. Bromine was purified through several freeze–pump–thaw cycles, and entrained in a controlled flow of N_2 through a bubbler held at 273 K in an ice bath to ensure a known and convenient vapour pressure. Oxygen was passed through a commercial electric-discharge Ozonisor to generate ozone.

4. Conditions, analysis, results

(a) CH_3OH enhancement of the HO_2 self-reaction rate

HO_2 radicals were formed following the broadband photolysis of $Cl_2/CH_3OH/O_2$ mixtures at 298 K and 760 Torr:

$$Cl_2 + h\nu \rightarrow 2Cl \quad (6)$$

$$Cl + CH_3OH \rightarrow HCl + CH_2OH \quad (7)$$

$$CH_2OH + O_2 \rightarrow HCHO + HO_2 \quad (8)$$

Concentrations of the reagents entering the reaction cell (given in Table 2) were sufficiently high to ensure rapid HO_2 formation with respect to its subsequent decay. Experiments were performed using the deuterium analysis lamp to provide low wavelength (<300 nm) light for absorption measurements. The optical acquisition conditions were 150 g per mm grating giving 130 nm coverage centered at 265 nm, and an entrance slit width of 500 μm corresponding to a spectral resolution (FWHM) of approximately 12 nm. The CCD was operated at a charge-transfer rate of 50 kHz, corresponding to a transfer time of 20 μs per row and a monitoring period of 0.016 s following photolysis.

Analysis of the resulting absorption spectra was complicated by the overlap and similarity of the HO_2 and H_2O_2 absorptions over the wavelength range analysed (210–260 nm): perfect deconvolution of these species contributions to the absorption spectra was not possible. The absorption spectra were therefore analysed by fitting just the HO_2 cross sections to the measured absorption spectra, and analysing the resulting decay traces using a model of the reaction system constructed in FACSIMILE, which included a correction for the erroneous retrieval of H_2O_2 as HO_2 in the fitting procedure. Such a correction was possible as the relationship between HO_2 and H_2O_2 was constrained in the model (by the stoichiometry of reaction (10)), and the magnitude of the correction was small—the absorption due to HO_2 accounted for more than 90% of the total absorption at all of the wavelengths considered, over the entire period of HO_2 decay. The reactions included in the model are listed in Table 3. Within the model, the initial Cl atom concentration and rate coefficient for the $HO_2 + HO_2$ reaction were optimised to minimise the sum of squares of residuals between calculated and observed decay traces. A typical decay trace and fit are shown in Fig. 2.

The values of k_{10} so obtained are listed in Table 4, as a function of [CH_3OH], and plotted in Fig. 3. Eqn. (ii), below (see

Table 2 Concentrations of precursor species in the reaction cell

Study	Precursor species concentration/molecule^{-1} cm^3					
	$Cl_2/10^{16}$	$Br_2/10^{15}$	O_2	$O_3/10^{16}$	$CH_3OH/10^{17}$	$CH_4/10^{18}$
(a) $HO_2 + HO_2$ experiments	2.5–6	—	1 atm	—	0.4–5.5	—
(b) Cl_2 photolysis calibration	1–6	—	1 atm	—	—	3
(c) $BrO + HO_2$ experiments	2.5–6	2.5–10	1 atm	2.5	1.2–3.3	—

discussion for derivation) was fitted to the data using a least squares analysis fitting technique:

$$k_{10} = \left(\frac{2.9 \times 10^{-12} + \alpha\beta[CH_3OH]}{(1 + \alpha[CH_3OH])^2} \right) \quad \text{(ii)}$$

α and β were found to be $(6.15 \pm 0.90) \times 10^{-19}$ molecule $^{-1}$ cm^3 and $(3.2 \pm 0.5) \times 10^{-11}$ molecule^{-1} cm^3 s^{-1} respectively. This parameterisation was used to determine the HO_2 self-reaction rate coefficient for the subsequent analysis of the $BrO + HO_2$ data. Also shown on Fig. 3 are the results and parameterisation of Andersson *et al.*[17]

(b) Actinometric calibration of Cl atom formation from Cl_2 photolysis

A knowledge of the photolytic dissociation of Cl_2 was required (as a function of chlorine concentration and flashlamp pulse energy) in order to permit determination of the initial HO_2 concentration in the $BrO + HO_2$ experiments. To determine this, Cl_2 photolysis was quantified by monitoring the formation of methylperoxy radicals following the photolysis of chlorine in the presence of excess methane and oxygen:

$$Cl_2 + h\nu \rightarrow 2Cl \quad (6)$$

$$Cl + CH_4 \rightarrow HCl + CH_3 \quad (11)$$

$$CH_3 + O_2 + M \rightarrow CH_3O_2 + M \quad (12)$$

Precursor concentrations (given in Table 2) were such that rapid and exclusive conversion of Cl atoms to CH_3O_2 was achieved. The optical conditions were identical to those used in the HO_2 self-reaction experiments described above, but with the CCD charge transfer interval set to 5 μs, corresponding to a total post-photolysis monitoring time of 0.004 s. This faster acquisition rate was chosen to minmise the chemical loss of CH_3O_2 in the decay traces, *via* its self-reaction:

$$CH_3O_2 + CH_3O_2 \rightarrow 2CH_3O + O_2 \quad (13a)$$

$$\rightarrow CH_2O + CH_3OH + O_2 \quad (13b)$$

$$\rightarrow CH_3OOCH_3 + O_2 \quad (13c)$$

Methylperoxy concentrations were obtained from the measured absorption at 260 nm, using an absorption cross section

Table 3 Reactions used in the HO_2 self-reaction model

Reaction	Rate coefficient/ molecule^{-1} cm^3 s^{-1} [a]
$Cl + CH_3OH \rightarrow HCl + CH_2OH$	5.4×10^{-11}
$CH_2OH + O_2 \rightarrow HCHO + HO_2$	9.1×10^{-12}
$HO_2 + HO_2 \rightarrow H_2O_2 + O_2$	Optimised
$Cl + HO_2 \rightarrow HCl + O_2$	3.2×10^{-11}
$Cl + HO_2 \rightarrow OH + ClO$	9.1×10^{-12}
$OH + HO_2 \rightarrow H_2O + O_2$	1.1×10^{-10}
$OH + H_2O_2 \rightarrow H_2O + HO_2$	1.7×10^{-12}
$ClO + HO_2 \rightarrow HOCl + O_2$	5.0×10^{-12}

[a] All from ref. 10.

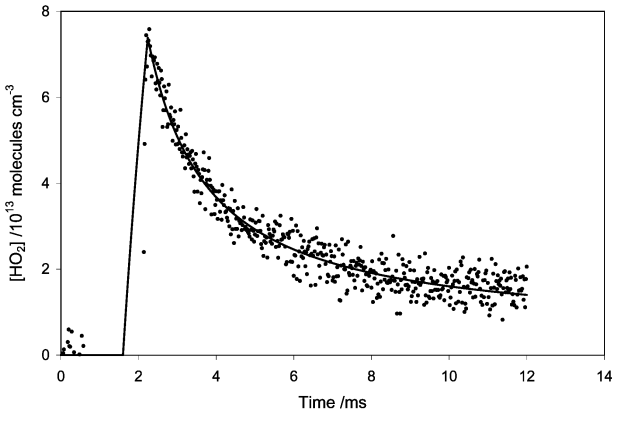

Fig. 2 HO_2 decay trace and optimised fit, $HO_2 + HO_2$ reaction system.

Table 4 Observed HO_2 self-reaction rate coefficient as a function of $[CH_3OH]$

$[CH_3OH]/10^{16}$ molecule cm^{-3}	$k_{obs}/10^{-12}$ molecule^{-1} cm^3 s^{-1} [a]
0.40	3.30 ± 0.27
1.29	4.69 ± 0.79
2.57	5.94 ± 0.89
3.10	6.18 ± 1.32
5.18	7.45 ± 1.13

[a] Errors are $\pm 2\sigma$ and represent (t-factor corrected) precision only.

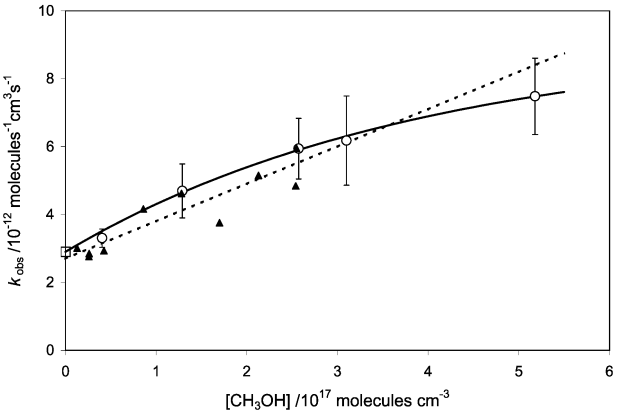

Fig. 3 HO_2 self-reaction rate coefficients as a function of $[CH_3OH]$: Circles and solid line: results and fit (eqn. (ii)) from this work; triangles and dashed line, results and fit of Andersson *et al.*;[17] Open square, zero methanol value from DeMore *et al.*[10]

of 3.26×10^{-18} molecule^{-1} cm^2.[10] The contribution to the total absorption at this wavelength (in the post- relative to pre-photolysis spectra) from the other absorbing species present (CH_3OOH, HO_2, H_2O_2 and HCHO) was always less than 0.6% of the total. The extent of Cl_2 photolysis was determined by fitting the measured CH_3O_2 decay traces using a simple model of the reaction system, consisting of reactions (11), (12) and (13), within which the initial Cl atom concentration and the overall methylperoxy self-reaction rate coefficient, k_{13}, were optimised. This fitting procedure was necessary in order to take into account the (slight) distortion imparted to the decay traces by the CCD time-averaging effect arising from the exposure of 31 rows of the device to incident light.

The initial Cl atom concentrations so obtained showed a linear increase with $[Cl_2]$ at a given flashlamp discharge voltage, as expected for the optically thin precursor gas mix. The $[Cl]/[Cl_2]$ relationship obtained was used to predict the initial HO_2 generation in the full $BrO + HO_2$ system. The returned value for k_{13} was $(4.0 \pm 1.0) \times 10^{-13}$ molecule^{-1} cm^3 s^{-1} (uncertainty is $\pm 2\sigma$). The relatively high imprecision reflects the small fraction of the peroxy radicals which underwent self-reaction over the monitoring period—which was selected to maximise sensitivity to the initial CH_3O_2 concentration. Nonetheless, this value is in agreement with the recommended value of $(4.7 \pm 1.5) \times 10^{-13}$ molecule^{-1} cm^3 s^{-1} from DeMore *et al.*[10]

(c) The BrO + HO_2 reaction

BrO and HO_2 radicals were formed following the flashlamp photolysis of chlorine and bromine in the presence of ozone, methanol and oxygen according to reactions (4)–(8). Precursor concentration ranges are given in Table 2. Experiments were performed using the xenon analysis lamp, under acquisition conditions of 300 g per mm grating, covering the wavelength range 308–372 nm, with a spectrograph entrance slit width of 100 μm, corresponding to a resolution of 1.41 nm (FWHM). The CCD was operated at a 2 μs charge transfer interval, giving a total post-flash monitoring period of 0.0016 s. Typically 20 photolysis shots were averaged per experiment.

The concentration of ozone present in the reaction cell was measured directly for each experimental run: Absorption spectra obtained during the pre-photolysis period, evaluated relative to the empty cell, were analysed by differential fitting of the structural features of the Huggins band between 316 and 338 nm to obtain the ozone concentration. The ozone cross sections used were recorded in separate experiments performed at the same resolution, with just O_2/O_3 present in the reaction cell, calibrated relative to the absorption at 253.65 nm in the Hartley band, using a cross section of 1.137×10^{-17} molecule^{-1} cm^2.[10]

BrO radicals were monitored *via* their characteristic structured UV-visible absorption spectra arising from the A $^2\Pi \leftarrow$ X $^2\Pi$ vibronic transition. Concentrations of BrO radicals were determined by fitting reference cross sections over the wavelength range 310–365 nm, using the technique of differential spectroscopy. The magnitude of the vibronic features manifest in the absorption spectra of species such as halogen monoxide radicals is dependent upon the instrumental resolution used, and the cross sections used to quantify such species must therefore be recorded at the appropriate resolution, or smoothed from higher resolution measurements. Wavelength-dependent BrO cross sections have been measured by Wahner *et al.*[21] Gilles *et al.*[22] subsequently re-measured the differential BrO cross section around 338 nm, and found it to be approximately 9% larger than that reported by Wahner *et al.* Gilles *et al.* noted that making a corresponding correction to rate coefficients for the BrO self-reaction measured *via* UV-absorption detection of BrO using the cross sections of Wahner *et al.* brought such results into agreement with those performed using other techniques. The BrO cross sections used in this work were those measured by Wahner *et al.*, increased in magnitude by 9% in line with the findings of Gilles *et al.*, and smoothed to the resolution used in this study.

The BrO concentration–time traces so obtained were analysed using a model of the reaction system constructed in FACSIMILE, incorporating the reactions given in Table 5. This reaction selection is discussed further within the sensitivity study section. Within the model, the ozone concentration obtained from the pre-flash absorption spectra was used, and methanol, bromine and chlorine concentrations were calculated from the appropriate flow rates and vapour pressures. The initial Cl atom concentration ($[Cl]_0 \equiv$ initial HO_2 concentration) and the HO_2 self-reaction rate coefficient were calculated from the chlorine and methanol concentrations. Initially, the photolytically generated Br atom concentration, $[Br]_0$, and the BrO + HO rate coefficient, k_1, were optimised to fit to the observed decay traces. However, we were unable to satisfactorily fit to the observed BrO decay traces using this approach. The observed traces could however be simulated well if the initial Cl atom concentration, $[Cl]_0$, were increased above that predicted on the basis of the actinometric calibration of the Cl_2 photolysis. This effect was attributed to the (potentially surface-mediated) disproportionation of Br_2 and Cl_2 in the gas manifold and reaction cell prior to photolysis, forming BrCl:

$$Br_2 + Cl_2 \Leftrightarrow 2BrCl \qquad (14)$$

$K_{14} = 10.1 \pm 1.1$ at 298 K.[23]

The absorption cross sections of BrCl are considerably larger than those of Cl_2 over the envelope of the UV-visible photolysis radiation, thus conversion of Cl_2 to BrCl followed by BrCl photolysis would enhance the Cl atom production above that anticipated from the chlorine concentration alone.

The model of the $BrO + HO_2$ chemical system was therefore altered to take account of this effect by including optimisation of $[Cl]_0$, in addition to $[Br]_0$ and k_1, and the $[Cl]_0/[Cl_2]$ calibration was used solely to provide the initial estimate for this parameter. The resulting simulated BrO decays were in good agreement with those measured, with optimised values for $[Cl]_0$ which were consistently higher than those predicted from

Table 5 Reactions included in the FACSIMILE optimisation model

Reaction	Rate/molecule^{-1} cm^3 s^{-1} [a]
$Br + O_3 \rightarrow BrO + O_2$	1.12×10^{-11}
$Cl + CH_3OH \rightarrow HCl + CH_2OH$	5.4×10^{-11}
$CH_2OH + O_2 \rightarrow HCHO + HO_2$	9.1×10^{-12}
$BrO + HO_2 \rightarrow HOBr + O_2$	a
$BrO + BrO \rightarrow 2Br + O_2$	2.7×10^{-12}
$BrO + BrO \rightarrow Br_2 + O_2$	4.8×10^{-13}
$HO_2 + HO_2 \rightarrow H_2O_2 + O_2$	b
$HO_2 + HCHO \rightarrow HOCH_2O_2$	8.15×10^{-14}
$HOCH_2O_2 \rightarrow HO_2 + HCHO$	108 c
$Br + HO_2 \rightarrow HBr + O_2$	2×10^{-12}
$Br + Br \rightarrow Br_2$	7.5×10^{-14}
$Cl + BrCl \rightarrow Br + Cl_2$	1.5×10^{-11}
$Cl + Br_2 \rightarrow BrCl + Br$	3.6×10^{-11}
$Cl + HO_2 \rightarrow HCl + O_2$	3.2×10^{-11}
$Cl + HO_2 \rightarrow OH + ClO$	9.1×10^{-12}
$Cl + O_3 \rightarrow ClO + O_2$	1.2×10^{-11}
$ClO + BrO \rightarrow Br + OClO$	6.8×10^{-12}
$ClO + BrO \rightarrow Cl + Br + O_2$	6.1×10^{-12}
$ClO + BrO \rightarrow BrCl + O_2$	1×10^{-12}
$ClO + HO_2 \rightarrow HOCl + O_2$	5×10^{-12}

[a] Notes: a—optimised; b—parameterised according to eqn. (ii); c—units s^{-1}. All rate coefficients from ref. 10.

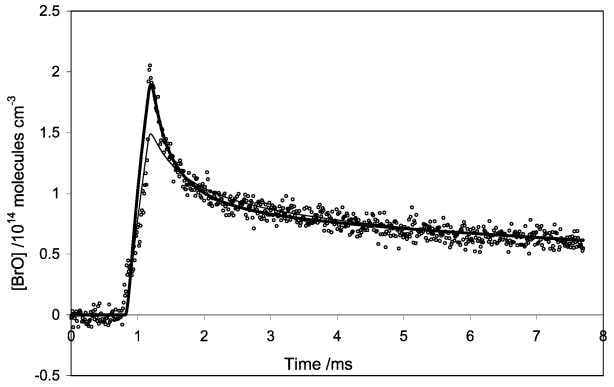

Fig. 4 BrO decay trace (points) and optimised fits: Fixing $[Cl]_0$ at value predicted by actinometric calibration, light line, and independently optimising $[Cl]_0$, heavy line.

the actinometric calibration. Examples of the fits obtained to a BrO decay trace with each of the models are shown in Fig. 4.

The values of k_1 obtained from this analysis are listed in Table 6, and plotted as a function of chlorine, bromine and methanol concentrations in Fig. 5. The mean value returned for the k_1, the overall $BrO + HO_2$ reaction rate coefficient at room temperature (295 ± 3 K) and pressure (760 ± 15 Torr) from 41 separate experiments was $(2.35 \pm 0.62) \times 10^{-11}$ molecule^{-1} cm^3 s^{-1}; uncertainty is 2 standard deviations and represents precision only. The optimised values of k_1 did not show any dependence (within uncertainty) upon the chlorine, bromine or methanol concentrations used, indicating that no unconsidered secondary chemical effects were occurring. Further confidence in the optimisation process was provided by the sensitivity test performed, discussed below.

5. Sensitivity analysis

In constructing the optimisation model (Table 5), a comprehensive set of reactions describing the $BrO + HO_2$ system was initially considered. This scheme was reduced by repeatedly fitting a decay trace and comparing the returned values of k_1 with each reaction in turn removed. Those which resulted in a change in the returned value of k_1 of less than 0.5% (when compared with the comprehensive reaction deck) were discarded—these were the various channels of the ClO self-reaction, including Cl_2O_2, OClO and subsequently Cl_2O_3 formation, the reactions of OH (formed from $Cl + HO_2$) with HO_2 and H_2O_2, the reactions of $HOCH_2O_2$ (formed *via* $HO_2 + HCHO$) with itself, BrO and HO_2.

The optimisation of k_1, $[Cl]_0$ and $[Br]_0$ within the model was tested as follows: A representative decay trace was repeatedly analysed, with each parameter in turn being perturbed from its optimal value, and the remaining two re-optimised. The deviation of the subsequent fits from the optimal trace was recorded as the sum of squares of residuals, calculated over the time period used within the optimisation model, this being the quantity minimised by the FACSIMILE optimisation routines to generate best-fit simulated traces. The resulting residual functions are shown in Fig. 6, in terms of the perturbation of each of the parameters. The presence of defined minima in each of the curves indicates that the 3 parameters were independently determined by the data. Unfortunately, the sensitivity to the $BrO + HO_2$ reaction rate coefficient is the least of the three, displaying the shallowest minimum. This is reflected in the lack of precision in the final determination of k_1.

The dependence of (the optimised values for) k_1 upon the rate coefficients used for the secondary reactions in the model was also assessed. A sample BrO decay trace was repeatedly analysed using the model, but with the rate coefficient for each reaction in turn increased and decreased by 50%. The percentage changes in the resulting values of k_1 relative to that obtained with the nominal rates are plotted in Fig. 7. The significant reactions can be seen to be $Br + O_3$, $BrO + BrO$ and $HO_2 + HO_2$.

Finally, the relative importance of the reactions included in the model is illustrated in Fig. 8, which shows the flux of primary reactant species ($[BrO] + [HO_2]$) through each reaction over the monitored period of the BrO decay. The $BrO + HO_2$ reaction dominates, followed by the BrO and HO_2 self-reactions. The only other secondary reactions of any significant sensitivity, $Br + HO_2$, $ClO + HO_2$ and $ClO + BrO$, are of comparatively minor importance, responsible for the loss of less than 1.5, 0.1 and 0.7% of the initial concentrations of BrO/HO_2 radicals respectively.

Table 6 Values of k_1 obtained as a function of $[Cl_2]$, $[Br_2]$ and $[CH_3OH]$, sorted by $[Cl_2]$

$[Cl_2]/10^{16}$ molecule cm^{-3}	$[Br_2]/10^{15}$ molecule cm^{-3}	$[CH_3OH]/10^{17}$ molecule cm^{-3}	$k_1/10^{-11}$ molecule^{-1} cm^3 s^{-1}
2.55	5.25	3.01	2.61
2.55	5.25	3.01	2.64
3.09	5.24	3.3	1.85
3.09	5.24	3.3	1.93
3.78	5.19	2.99	2.49
3.78	5.19	2.99	2.48
3.78	5.19	2.99	2.22
3.78	5.19	2.99	2.55
4.77	10.12	3.34	2.58
4.77	10.12	3.34	2.32
4.77	10.12	3.34	1.83
4.77	5.06	3.34	2.77
4.77	5.06	3.34	2.62
4.77	7.59	3.34	2.52
4.77	7.59	3.34	2.7
4.77	2.53	3.34	2.87
4.77	7.59	3.34	2.5
4.77	5.06	3.34	2.91
4.86	5.16	3.25	2.26
4.86	5.16	3.25	1.82
4.86	5.16	3.25	2.27
4.86	5.16	3.25	2.2
4.86	5.16	3.25	1.94
4.86	5.16	3.25	2.65
4.9	5.11	3.3	2.12
4.9	5.11	3.3	2.23
4.9	5.11	3.3	2.34
4.9	5.11	3.3	2.15
4.99	5.14	2.96	2.22
4.99	5.14	2.96	2.4
4.99	5.14	2.96	2.27
4.99	5.14	2.96	2.29
5.09	5.31	2.15	2.11
5.09	5.31	2.15	2.62
5.24	5.46	1.24	2.23
5.24	5.46	1.24	2.88
6.02	5.11	3.22	1.72
6.17	5.08	2.93	2.45
6.17	5.08	2.93	2.59
6.17	5.08	2.93	2
6.17	5.08	2.93	2.13

6. Discussion

$HO_2 + HO_2$ methanol enhancement

Hamilton and Lii[18] and Kircher and Sander[24] observed a linear increase in k_{10} (k_{obs}) with respect to water concentration,

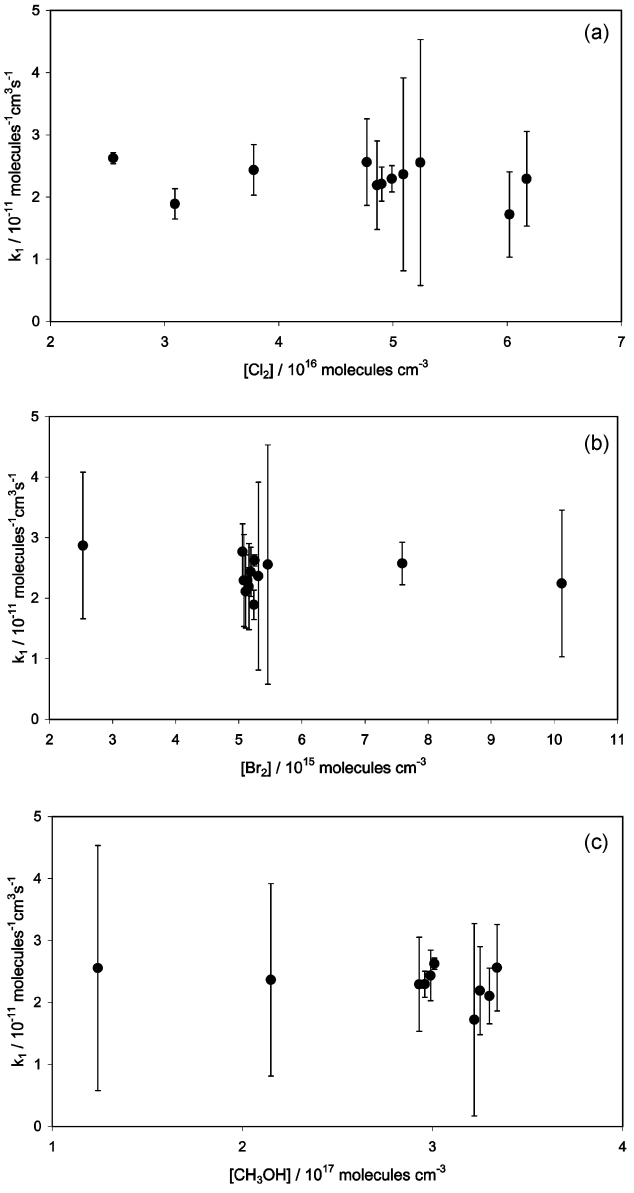

Fig. 5 Dependence of k_1 upon (a) chlorine, (b) bromine and (c) methanol concentration. Error bars correspond to product of the standard deviation and the 95% certainty students *t*-factor for the number of observations at each precursor concentration.

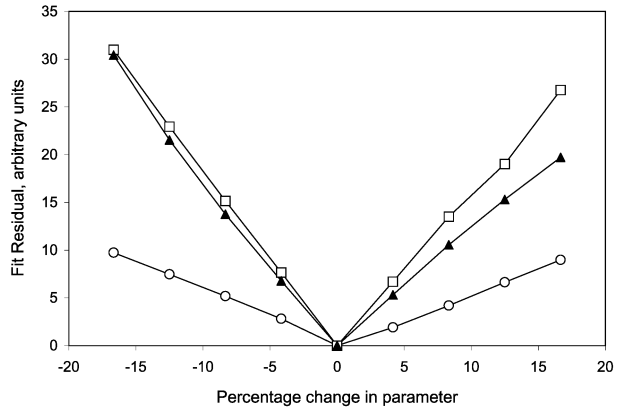

Fig. 6 Sensitivity of BrO decay traces to $[Cl]_0$, $[Br]_0$ and k_1. Residuals obtained when each parameter is perturbed from its optimal value, and the remaining two are re-optimised. Open squares, $[Cl]_0$; filled triangles, $[Br]_0$; open circles, k_1.

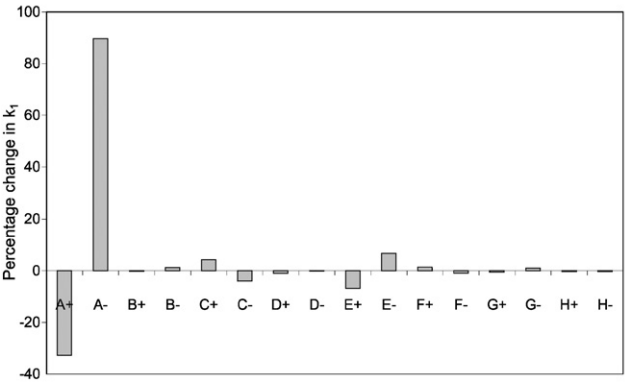

Fig. 7 Sensitivity of the returned value of k_1 to the rate coefficients for the secondary reactions employed in the optimisation model. Figure shows percentage change in k_1 for a 50% increase or decrease in each secondary reaction rate coefficient. Reaction key: +/− indicates rate coefficient increased/decreased; A: $Br + O_3$, B: $Cl + CH_3OH$, C: $BrO + BrO$, D: $Br + HO_2$, E: $HO_2 + HO_2$, F: $Cl + O_{3+}$, G: $ClO + HO_2$, H: $Cl + HO_2$. Also considered but not shown (all less than 1%): $CH_2OH + O_2$, $Br + Br + M$, $ClO + BrO$.

up to $[H_2O] = 4.5 \times 10^{17}$ molecule cm^{-3}. Andersson *et al.*[17] reported a similar linear increase in k_{obs} in the presence of methanol, up to $[CH_3OH] = 2.5 \times 10^{17}$ molecule cm^{-3}. However, (in the presence of ammonia) Hamilton and Lii and Lii *et al.*[19] found that the observed rate coefficient initially increased in a linear fashion with respect to $[NH_3]$, but that at high concentrations ($[NH_3] > 2 \times 10^{17}$ molecule cm^{-3}) the rate enhancement fell off, and at NH_3 concentrations over 4×10^{17} molecule cm^{-3} the apparent reaction rate decreased with increasing $[NH_3]$ (at 298 K). These observations may be explained *via* a chaperone mechanism, in which the additional species (H_2O, NH_3 or CH_3OH) hydrogen-bonds to the HO_2 radicals, facilitating formation of H_2O_2. Under the conditions of this work (no pressure or temperature dependence investigated), the methanol-dependence observed may be explained by the following simple mechanism:

$$HO_2 + HO_2 \rightarrow H_2O_2 + O_2 \quad (10)$$

$$HO_2 + CH_3OH \leftrightarrow CH_3OH \cdots HO_2 \quad (15)$$

$$CH_3OH \cdots HO_2 + HO_2 \rightarrow CH_3OH + H_2O_2 + O_2 \quad (16)$$

Following Hamilton and Lee,[18] if the equilibrium in reaction (15) is rapid, and the absorption cross section of $CH_3OH \cdots HO_2$ is equal to that of HO_2 over the wavelengths monitored, the rate of reaction of the observed quantity, $(HO_2 + CH_3OH \cdots HO_2)$, is given by:

$$-\frac{d([HO_2] + [CH_3OH \cdots HO_2])}{dt} = 2k_{10}[HO_2]^2 + 2k_{16}K_{15}[HO_2]^2[CH_3OH] \quad \text{(iii)}$$

Where K_{15} is the equilibrium constant for reaction (15). The observed rate constant for HO_2 loss, k_{obs}, is then defined by:

$$k_{obs} = \frac{d([HO_2] + [CH_3OH \cdots HO_2])}{2([HO_2] + [CH_3OH \cdots HO_2])^2 dt} \quad \text{(iv)}$$

and hence is given by:

$$k_{obs} = \frac{k_{10} + k_{16}K_{15}[CH_3OH]}{(1 + K_{15}[CH_3OH])^2} \quad \text{(v)}$$

At the highest methanol concentrations used in this study, a fall off in the enhancement of the HO_2 self-reaction rate is observed, and hence the data was fitted using eqn. (v), with k_{10}, the self-reaction rate in the absence of methanol, fixed at 2.9×10^{-12} molecule^{-1} cm^3 s^{-1}. The values obtained

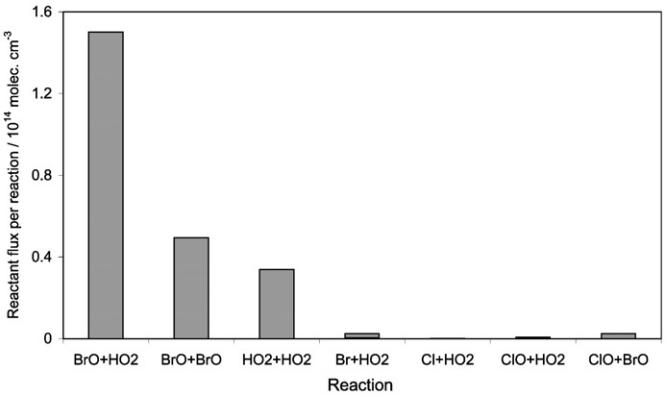

Fig. 8 Integrated total of reactant species ($= [BrO] + [HO_2]$) consumed by each reaction during the monitored decay period.

were $K_{15} = (6.15 \pm 0.90) \times 10^{-19}$ molecule^{-1} cm^3 and $k_{16} = (3.2 \pm 0.5) \times 10^{-11}$ molecule^{-1} cm^3 s^{-1}.

In the previous study of Andersson *et al.*,[17] no curvature in the plot of observed self-reaction rate *vs.* methanol was observed over the lower concentration ranges investigated (Fig. 3), and their data were parameterised by eqn. (vi):

$$k_{obs} = (2.7 \pm 0.6) \times 10^{-12} + (1.1 \pm 0.4) \times 10^{-29} \times [CH_3OH] \quad \text{(vi)}$$

This parameterisation would correspond to the case where $K_{15}[CH_3OH] \ll 1$, thus the parameters obtained by Andersson *et al.* ($\equiv k_{10}$ and $k_{16}K_{15}$) are not directly comparable to the results of this work.

BrO + HO$_2$ reaction rate coefficient

The rate coefficient for the $BrO + HO_2$ reaction obtained in this work is compared with other (298 K) measurements in Table 1. The most likely causes of disagreement between this work and the previous studies lie in the use of a complex reaction model to infer $[HO_2]$ and to account for the consumption of the reactant species through secondary chemical reactions, principally $BrO + BrO$ and $HO_2 + HO_2$. However, the sensitivity study (Fig. 7) shows that the BrO formation chemistry has the greatest impact upon the returned value of k_1, followed by the $HO_2 + HO_2$ and $BrO + BrO$ reactions, both of which have been explicitly considered in this and previous studies. The rate coefficient for the $Br + O_3$ reaction is well known at 298 K, the ozone concentration present in the experiments was directly determined for each experimental run, and the initial concentration of Br atoms was optimised (in effect determined by the initial BrO concentration), thus the error in calculation of the $Br + O_3$ reaction rate within the model is expected to have been small. Moreover, when the rate coefficient for this reaction was perturbed in the sensitivity study, the fits obtained to the BrO data were much worse than those obtained with the accepted value—indicating that the correct concentrations and rates were being used.

We estimate the uncertainty in the determination of $[O_3]$ to be less than 5%, and in the $Br + O_3$ reaction rate to be of the order of 20%.[10] Taking the variation in the BrO cross sections obtained by Wahner *et al.*[21] and Gilles *et al.*[22] (10%) as indicative of their relative accuracy, a systematic error estimate (in the determination of k_1) of the order of 23% is obtained, which when combined with the (2σ) statistical error gives k_1, 298 K $= (2.35 \pm 0.82) \times 10^{-11}$ molecule^{-1} cm^3 s^{-1}.

Of the various measurements of k_1 reported, the results of Cox and Sheppard[2] are not compatible with any of the subsequent studies, and are not considered further here. The remaining literature datasets fall into two geographically defined groups, the "low" rates measured in the USA, and the "high" measurements obtained in France. The value obtained in the current work lies between these groups, and is in best agreement with the measurements of Li *et al.*[7] (1.9 ± 0.6) and Cronkhite *et al.*[8] (2.0 ± 0.6), although the range from this work also encompasses the mean value from the most recent study of Bedjanian *et al.*[9] (3.1 ± 0.8). The lower value of Elrod *et al.*[6] (1.4 ± 0.3) is also in agreement when the combined uncertainties are considered (all values in units of 10^{-11} molecule^{-1} cm^3 s^{-1}).

Bridier *et al.*[4] used the same chemical system and flash photolysis technique as in this work, with BrO and HO_2 concentrations determined through single-wavelength UV absorption at 313/329 and 210/220 nm respectively. However, under the conditions employed, ozone would have made a much larger contribution to the low wavelength absorption than HO_2, potentially resulting in uncertainties in the derived $[HO_2]$: In the current work, to a first approximation, underestimation of the HO_2 concentration would result in an overestimate of k_1. The first experiments conducted by the Orleans groups[3,5] used a discharge flow/mass spectrometry system to study reaction (1), under conditions of excess HO_2. HO_2 radicals were generated *via* the $Cl/CH_3OH/O_2$ method, and quantified by titration with NO and subsequent detection of NO_2, while the (minor reagent) BrO was formed through the $O + Br_2$ reaction. This system was subject to some problems with heterogeneous interactions affecting the HO_2 generation, especially at the lower temperatures studied, the effect of which were to increase the returned values for k_1.

Li *et al.*[7] used a similar discharge flow/mass spectrometry technique to study the reaction, with both BrO and (separately) HO_2 in excess, obtaining results which agreed to within 20%. Li *et al.* employed a heated injector for HO_2 admission to circumvent some of the problems encountered by Larichev *et al.*[5] at lower temperatures, however it is not clear that this should have significantly affected the rate measured at 298 K.

The study of Elrod *et al.*[6] was conducted at intermediate pressures (*ca.* 100 Torr) using the turbulent discharge-flow technique, with BrO radicals (from $O + Br_2$) undergoing reaction with excess HO_2 (from $H + O_2$), which was quantified *via* NO titration. The value determined, $(1.4 \pm 0.3) \times 10^{-11}$ molecule^{-1} cm^3 s^{-1}, is lower than the other measurements performed recently; the authors note that in the studies of Cox and Sheppard[2] and of Li *et al.*,[7] in which k_1 was measured under conditions of both HO_2 and BrO in excess, the values for k_1 were lower with excess HO_2.

Cronkhite *et al.*[8] utilised a similar chemical scheme to that employed in this work, with 308 nm laser photolysis of O_3 and Cl_2 leading to reactant formation. BrO radicals were monitored *via* UV absorption spectroscopy, while HO_2 was monitored simultaneously using a tunable diode laser. The HO_2 concentration determination was thus not susceptible to the potential wall loss problems of some of the previous studies.

Experiments were performed under pseudo first-order conditions, with HO_2 in excess over BrO, at pressures of 12 and 25 Torr. The principal uncertainty in the value obtained, $(2.0 \pm 0.6) \times 10^{-11}$ molecule^{-1} cm^3 s^{-1} arose from the infrared line strengths used to quantify HO_2. Finally, Bedjanian *et al.*[9] also used discharge flow/mass spectrometry techniques to study reaction (1). Experiments were performed with both HO_2 and BrO in excess, with BrO radicals generated from $O + Br_2/Br + O_3$ and HO_2 radicals from $F + H_2O_2$. A dual sliding-injector arrangement was used to minimise wall loss of the excess reagent, which occurred (albeit to a limited extent) in the previous flow-tube studies. Results from both pseudo-first-order systems were in good agreement. In addition Bedjanian *et al.* performed a relative rate measurement, in which Br atoms and BrO radicals competed for reaction with HO_2. The production of HOBr was monitored as a function of the initial Br:BrO ratio (BrO_x present in excess), determining a value of k_1, 298 K of $(2.95 \pm 0.80) \times 10^{-11}$ molecule^{-1} cm^3 s^{-1} relative to the rate of the reaction $Br + HO_2 \rightarrow HBr + O_2$.

Atmospheric implications

The $BrO + HO_2$ cycle is one of many intercoupled catalytic ozone destruction cycles; as such the impact of one particular kinetic parameter upon the evolution of ozone levels can only be accurately quantified through the use of numerical models. Qualitatively we expect ozone loss through the $BrO + HO_2$ cycle to reflect changes in the value of k_1, although calculated total ozone loss may be reduced, if, for example, greater flux through the $BrO + HO_2$ reaction reduces the available BrO and hence the impact of competing cycles such as $BrO + ClO$. The JPL 97-4 evaluation (DeMore *et al.*[10]) gives a value for the $BrO + HO_2$ reaction rate coefficient of $k_1 = 3.4 \times 10^{-12} \exp((540 \pm 200)/T)$ molecule^{-1} cm^3 s^{-1}, corresponding to a value of $(2.1 \pm 1.5) \times 10^{-11}$ molecule^{-1} cm^3 s^{-1} at 298 K. The result from this study, $k_1 = (2.35 \pm 0.82) \times 10^{-11}$ molecule^{-1} cm^3 s^{-1}, is about 10% higher, implying slightly greater ozone loss through the $BrO + HO_2$ cycle if this factor is maintained down to stratospheric temperatures.

There is still considerable uncertainty over the 298 K rate coefficient for the $BrO + HO_2$ reaction. The JPL 97-4 evaluation is based upon the results of Larichev *et al.*,[5] Elrod *et al.*[6] and Li *et al.*[7] While potential problems have been identified with some of the earlier studies of this reaction, no obvious reasons have been identified for the discrepancy between the results of Elrod *et al.*, Li *et al.*, and Cronkhite *et al.*,[8] and those of Bedjanian *et al.*[9] at 298 K. The results of this work confirm that k_1, 298 K lies within the approximate range $(2–3) \times 10^{-11}$ molecule^{-1} cm^3 s^{-1} but are not sufficiently precise to discriminate between the "low" and "high" groups of measurements.

Acknowledgement

WJB and DMR thank the NERC for award of a studentship and advanced research fellowship respectively. This work was supported through the European Commission Environment and Climate Program (COBRA-ENV-CT97-0576).

References

1 Y. L. Yung, J. P. Pinto, R. T. Watson and S. P. Sander, *J. Atmos. Sci.*, 1980, **37**, 339.
2 R. A. Cox and D. W. Sheppard, *J. Chem. Soc., Faraday Trans. 2*, 1982, **78**, 1383.
3 G. Poulet, M. Pirre, F. Maguin, R. Ramaroson and G. Le Bras, *Geophys. Res. Lett.*, 1992, **19**, 2305.
4 I. Bridier, B. Veyret and R. Lesclaux, *Chem. Phys. Lett.*, 1993, **201**, 563.
5 M. Larichev, F. Maguin, G. Le Bras and G. Poulet, *J. Phys. Chem.*, 1995, **99**, 15 911.
6 M. J. Elrod, R. F. Meads, J. B. Lipson, J. V. Seeley and M. J. Molina, *J. Phys. Chem.*, 1996, **100**, 5808.
7 Z. Li, R. R. Friedl and S. P. Sander, *J. Chem. Soc., Faraday Trans.*, 1997, **93**, 2683.
8 J. M. Cronkhite, R. E. Stickel, J. M. Nicovich and P. H. Wine, *J. Phys. Chem. A*, 1998, **102**, 6651.
9 Y. Bedjanian, V. Riffault and G. Poulet, *J. Phys. Chem. A*, 2001, **105**, 3167.
10 W. B. DeMore, S. P. Sander, D. M. Golden, R. F. Hampson, M. J. Kurylo, C. J. Howard, A. R. Ravishankara, C. E. Kolb and M. J. Molina, *Chemical Kinetics and Photochemical Data for Use in Stratospheric Modelling*, JPL Publication 97-4, 1997.
11 D. J. Lary, *J. Geophys. Res.*, 1996, **101**, 1505.
12 R. R. Garcia and S. Solomon, *J. Geophys. Res.*, 1994, **99**, 12 937.
13 A. Mellouki, R. K. Talukdar and C. J. Howard, *J. Geophys. Res.*, 1994, **99**, 22 949.
14 N. Kaltsoyannis and D. M. Rowley, *Phys. Chem. Chem. Phys.*, 2002, **4**, 419.
15 R. Vogt, P. J. Crutzen and R. Sander, *Nature*, 1996, **383**, 327.
16 D. M. Rowley, M. H. Harwood, R. A. Freshwater and R. L. Jones, *J. Phys. Chem.*, 1996, **100**, 3020.
17 B. Y. Andersson, R. A. Cox and M. E. Jenkin, *Int. J. Chem. Kinet.*, 1988, **20**, 283.
18 E. J. Hamilton and R. Lii, *Int. J. Chem. Kinet.*, 1977, **9**, 875.
19 R. Lii, R. A. Gorse, M. C. Sauer and S. Gordon, *J. Phys. Chem.*, 1980, **84**, 813.
20 A. R. Curtis and W. P. Sweetenham, FACSIMILE, AERE Harwell Publication R 12805, Computer Science and Systems Division, Harwell Laboratory, Oxfordshire, UK, 1987.
21 A. Wahner, A. R. Ravishankara, S. P. Sander and R. R. Friedl, *Chem. Phys. Lett.*, 1988, **152**, 507.
22 M. K. Gilles, A. A. Turnipseed, J. B. Burkholder, A. R. Ravishankara and S. Solomon, *J. Phys. Chem.*, 1997, **101**, 5526.
23 D. Maric, J. P. Burrows and G. K. Moortgat, *J. Photochem. Photobiol. A: Chem.*, 1994, **83**, 179.
24 C. C. Kircher and S. P. Sander, *J. Phys. Chem.*, 1984, **88**, 2082.